Multi-plane lensing in wave optics

Job Feldbrugge[1, 2, *]

[1]*Perimeter Institute, 31 Caroline St N, Waterloo, ON N2L 2Y5, Canada*
[2]*Carnegie Mellon University, 5000 Forbes Ave, Pittsburgh, PA 15217, USA*

Wave effects in lensing form a rich field on the intersection of classical caustic singularities and quantum interference, yet are notoriously difficult to model. I present a new method to define and efficiently evaluate multi-plane lensing of coherent electromagnetic waves by plasmas and gravitational lenses in polynomial time. The large number of recently observed pulsars and fast radio bursts in radio astronomy suggest that wave effects will likely be observed in the near future. The interference fringes are sensitive to physical parameters which cannot be inferred from geometric optics. In particular, for multi-plane lensing, the pattern depends on the redshifts of the lens planes. The study of these effects will allow the use of radio sources to probe our universe in novel ways.

Lensing is of key importance in astronomy and cosmology, as it allows us to infer properties of lenses which cannot be seen in other ways. For example, gravitational microlensing allows us to detect faint but massive foreground objects, including exoplanets, and to put tight constraints on their contribution to the dark matter [1–6]. Plasma lenses have been observed to amplify astronomical signals, such as the "Black Widow" pulsar [7]. The turbulent interstellar medium leads to scintillation effects [8–10]. Radiation often propagates through multiple lenses before reaching us. When the lenses are widely separated in the radial direction, this leads to an important effect that we shall quantify here.

In astronomy, lensing is usually considered in the limit of geometric optics, in which light travels along null geodesics and the image is determined by the geometry of the light rays [11–13]. This is an excellent approximation when the wavelength of the radiation is short compared to the characteristic lensing scale, if the source is extended, and if the radiation is incoherent. Nevertheless, there are cases in which the geometric optics approximation fails. For pulsars and fast radio bursts (FRBs), the wave nature of the radiation can become important, as these sources are very small and their radio emissions are coherent. While we have yet to observe interference fringes in gravitational lensing, scintillation by plasma lenses is detected on a regular basis.

The observation of wave effects in lensing opens a new window for astronomy, as the diffraction pattern of a lens is significantly richer than the corresponding intensity pattern in geometric optics. Unlike the latter, the diffraction pattern depends on the frequency in a way that can be used to constrain the system's physical parameters. For example, the diffraction patterns in the lensing of gamma ray bursts (GRBs) have been proposed as a probe to constrain possible dark matter candidates [14, 15]. It was recently demonstrated that wave effects generally increase the cross section for lensing events and allow us to put tight constraints on the mass of a gravitational point lens [16]. Likewise, the diffraction pattern of a binary gravitational lens strongly depends on the individual masses of the gravitating bodies [17]. The detection of fringes in the lensing of FRBs can tightly constrain the abundance of dark matter in the form of massive astrophysical compact halo objects (MACHOs) [18]. In this letter, I show that, unlike the geometric optics intensity, the fringes in multi-plane lensing allow one, in principle, to determine the redshifts of the lens planes.

In the coming years, telescopes such as the Canadian Hydrogen Intensity Mapping Experiment (CHIME) [19], the Hydrogen Intensity and Real-time Analysis eXperiment (HIRAX) [20], and the Square Kilometer Array (SKA) [21], as well as next-generation follow-ups including the Canadian Hydrogen Observatory and Radio-transient Detector (CHORD) [22] and the Packed Ultra-wideband Mapping Array

---

* jfeldbrugge@perimeterinstitute.ca

(PUMA) [23] will detect large numbers of coherent radio sources on the sky [24]. Improving our understanding of wave effects in gravitational and plasma lensing will allow us to take advantage of these observations.

Wave effects in optics have traditionally been studied with the semi-classical or Eikonal approximation. This approximation is an improvement over the geometric approximation, as it captures the interference between different images. However, the approximation fails near caustics where the intensity diverges. In contrast, the full wave-optics picture is determined by a path integral over all possible paths between the source and observer [25]. In the thin-lens approximation, this path integral reduces to the astronomical Kirchhoff-Fresnel integral. This highly oscillatory integral is unfortunately delicate to define and difficult to evaluate. In a recent paper, we used Cauchy's theorem in multi-dimensional complex analysis (Picard-Lefschetz theory [26]) to provide a rigorous definition of and to efficiently evaluate the single-plane lens integral [27]. For more details on this method and a numerical implementation, see [28]. In this letter, I extend the definition and the evaluation method to multi-plane lenses, which are more realistic. I express the high-dimensional lens integral as an iterated integral defined using analytic methods. Moreover, I propose an efficient scheme combining Picard-Lefschetz theory and the Eikonal method which terminates in polynomial time. This is the first time that we are able to study multi-plane lensing in the full wave-optics regime.

In this letter, I first summarize multi-plane lensing in geometric optics, before presenting the corresponding wave optics analysis. I express the wave optics integrals in terms of an analytic and a multi-image part and use complex analysis and Fast Fourier Transforms to evaluate these parts. Finally, I demonstrate the merit of this new integration scheme with a double-plane plasma lens model and two gravitational lens models.

Geometric optics: Consider radiation traveling through n discrete lens-planes L_i, $i = 1, \ldots, n$, at redshifts z_i separating the observer from the source (such that $0 \leq z_1 \leq \cdots \leq z_n$). Let d_{ij} be the angular diameter distance be-
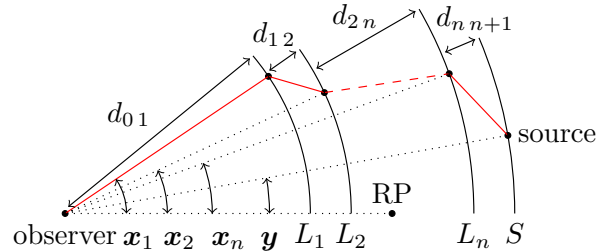

Figure 1: Geometry of interfering paths in a multi-plane lens system (reference point RP).

tween the lens-spheres L_i and L_j, and $\boldsymbol{x}_i$ the angular coordinate of the intersection of a light ray with the lens-plane L_i, with respect to the coordinate system centered on the observer (see Fig. 1). Let $\boldsymbol{y} = \boldsymbol{x}_{n+1}$ be the position at which the light ray intersects the source-plane $S = L_{n+1}$. In [11], the ray optics is completely determined by the time-delay function (relative to the unperturbed trajectory)

$$T(\boldsymbol{x}_1, \ldots, \boldsymbol{x}_{n+1}) = \sum_{i=1}^{n} T_i(\boldsymbol{x}_i, \boldsymbol{x}_{i+1}), \quad (1)$$

with the time-delay $T_i(\boldsymbol{x}_i, \boldsymbol{x}_{i+1})$ between planes L_i and L_{i+1} given by

$$(1+z_i)\frac{d_{0\,i}d_{0\,i+1}}{c\,d_{i\,i+1}}\left[\frac{(\boldsymbol{x}_i - \boldsymbol{x}_{i+1})^2}{2} + \beta_{i\,i+1}\varphi_i(\boldsymbol{x}_i)\right]. (2)$$

The first term is the Pythagorean contribution, corresponding to the variations in the path length. The second is the time-delay due to a gravitational- or plasma-induced phase φ_i, received while passing through the i-th lens-plane, weighted by the geometric coefficient

$$\beta_{ij} = \frac{d_{i\,j}d_{0\,n+1}}{d_{0\,j}d_{i\,n+1}}. \quad (3)$$

Given a surface mass density Σ_i, the gravitational phase variation $\varphi_i(\boldsymbol{x}_i)$ is given by

$$-\frac{4G}{c^2}\frac{d_{0\,i}d_{i\,n+1}}{d_{0\,n+1}}\int \Sigma_i(\boldsymbol{x})\log\|\boldsymbol{x}_i - \boldsymbol{x}\|\mathrm{d}\boldsymbol{x}, \quad (4)$$

with Newton's constant G. For a plasma with an electron density $\Sigma_{i,e}$ on L_i, the phase variation is

$$\varphi_i(\boldsymbol{x}_i) = -\frac{d_{0\,i}d_{i\,n+1}}{d_{0\,n+1}}\frac{\Sigma_{i,e}(\boldsymbol{x}_i)e^2}{m_e\,\epsilon_0\,\omega^2}, \quad (5)$$

with the electron mass m_e and charge e, the vacuum permittivity ϵ_0 and the frequency of the radiation ω. (We assume the speed of light in vacuum $c = 1$.)

Fermat's principle states that we observe images along rays for which the arrival time is an extremum. Applying this to the time-delay function (1), we obtain the conditions

$$\boldsymbol{x}_{i+1} - \boldsymbol{x}_i = -\,(1 + z_{i-1})\frac{d_{0\,i-1}d_{i\,i+1}}{d_{0\,i+1}d_{i-1\,i}}\,(\boldsymbol{x}_{i-1} - \boldsymbol{x}_i) \\ + \beta_{i\,i+1}\boldsymbol{\alpha}_i\,(\boldsymbol{x}_i)\,, \quad i = 1, \ldots, n \quad (6)$$

with $\boldsymbol{x}_0 = \boldsymbol{0}$, and the deflection angle $\boldsymbol{\alpha}_i \equiv \nabla\varphi_i$. This iterative equation is solved by

$$\boldsymbol{x}_j = \boldsymbol{x}_1 + \sum_{i=1}^{j-1} \beta_{i\,j}\boldsymbol{\alpha}_i(\boldsymbol{x}_i), \; j = 2, \ldots, n+1. \quad (7)$$

It induces a Lagrangian map $\boldsymbol{\xi} : L_1 \to S$ that expresses the intersection of the ray with the source-plane in terms of the angle on the sky,

$$\boldsymbol{\xi}(\boldsymbol{x}_1) = \boldsymbol{x}_1 + \sum_{i=1}^{n} \beta_{i\,j}\boldsymbol{\alpha}_i(\boldsymbol{x}_i). \quad (8)$$

Note that geometric optics is completely determined by the geometric coefficients $\beta_{i\,j}$ and the deflection angles $\boldsymbol{\alpha}_i$. It does not depend on the redshifts z_i of the lens-planes.

In geometric optics, the deformation tensor $\mathcal{D} = \nabla_{\boldsymbol{x}_1}\boldsymbol{\xi}$ determines the lensing pattern. Whereas the deformation tensor of a single-plane lens ($n = 1$) is symmetric, including a shear and a magnification term, the deformation tensor of the multi-plane lens is generically not symmetric. The intensity of the image is given by

$$I_{geom}(\boldsymbol{\mu}) = \sum_{\boldsymbol{x}_1 \in \boldsymbol{\xi}^{-1}(\boldsymbol{\mu})} \frac{1}{|\det \nabla_{\boldsymbol{x}_1}\boldsymbol{\xi}(\boldsymbol{x}_1)|} \quad (9)$$

which spikes on the caustic network $\mathcal{C} = \boldsymbol{\xi}(\mathcal{M})$ with the critical curve

$$\mathcal{M} = \{\boldsymbol{x}_1 \in L_1 \mid \det \nabla_{\boldsymbol{x}_1}\boldsymbol{\xi}(\boldsymbol{x}_1) = 0\}\,. \quad (10)$$

A wave analysis is required to understand the intensity near these caustics, as the geometric optics and the Eikonal approximations fail in these regions. For a detailed discussion of caustics and their classification by Lagrangian catastrophe theory, see [29–31].

Wave optics: In wave optics, the lens pattern is again determined by the time-delay function, but this time through the Kirchhoff-Fresnel path integral

$$\Psi[\boldsymbol{y}] = \mathcal{N} \int_{(\mathbb{R}^d)^n} e^{i\omega T(\boldsymbol{x}_1, \ldots, \boldsymbol{x}_n, \boldsymbol{y})}\mathrm{d}\boldsymbol{x}_1 \ldots \mathrm{d}\boldsymbol{x}_n, \quad (11)$$

taken over paths which are piecewise linear between the lens planes. The frequency is ω and the dimension of the lens-planes is d. The integral is normalized by

$$\mathcal{N} = \left(\frac{\omega}{2\pi i}\prod_{i=1}^{n}(1 + z_i)\frac{d_{0\,i}d_{0\,i+1}}{d_{i\,i+1}}\right)^{nd/2}, \quad (12)$$

so that the intensity $I(\boldsymbol{y}) = |\Psi(\boldsymbol{y})|^2$ is unity in the absence of a lens, i.e., $I(\boldsymbol{y}) = 1$ when $\varphi_i = 0$ for all i.

The highly oscillatory nd-dimensional integral Ψ is unfortunately difficult to define and expensive to evaluate. For this reason, we express it as an iterated integral

$$\Psi_{i+1}(\boldsymbol{x}_{i+1}) = \mathcal{N}_i \int_{\mathbb{R}^d} \Psi_i(\boldsymbol{x}_i)e^{i\omega T_i(\boldsymbol{x}_i, \boldsymbol{x}_{i+1})}\mathrm{d}\boldsymbol{x}_i \quad (13)$$

for $i = 1, \ldots, n$, with the initial wave function $\Psi_1(\boldsymbol{x}_1) = 1$, the final amplitude $\Psi(\boldsymbol{y}) = \Psi_{n+1}(\boldsymbol{y})$, and the normalization factors

$$\mathcal{N}_i = \left(\frac{\omega}{2\pi i}(1 + z_i)\frac{d_{0\,i}d_{0\,i+1}}{d_{i\,i+1}}\right)^{d/2}. \quad (14)$$

Now using Cauchy's integral theorem, we deform the integration domain into the complex plane. For the first integral, $\Psi_2(\boldsymbol{x}_2)$, we deform the integration domain $\mathbb{R}^d$ to the Lefschetz thimble $\mathcal{J}_1 \subset \mathbb{C}^d$ along which the integrand becomes monotonically decreasing,

$$\Psi_2(\boldsymbol{x}_2) = \mathcal{N}_1 \int_{\mathcal{J}_1} e^{i\omega T_1(\boldsymbol{x}_1, \boldsymbol{x}_2)}\mathrm{d}\boldsymbol{x}_1, \quad (15)$$

and is absolutely convergent, removing any ambiguities (for a detailed discussion of Picard-Lefschetz theory, see [26]). For local lenses, away from the caustics, the dominant relevant saddle point is given by the unperturbed ray $\boldsymbol{x}_1 = \boldsymbol{x}_2$, hence

$$\Psi_2(\boldsymbol{x}_2) \approx e^{i\omega T_1(\boldsymbol{x}_2, \boldsymbol{x}_2)} \quad (16)$$

(a) $I(\boldsymbol{x}_2) = |\Psi_2(\boldsymbol{x}_2)|^2$ (b) $I(\boldsymbol{x}_3) = |\int_{\mathbb{R}^d} e^{i\omega(T_1+T_2)}\mathrm{d}\boldsymbol{x}_2|^2$ (c) $I(\boldsymbol{x}_3) = |\Psi_3(\boldsymbol{x}_3)|^2$
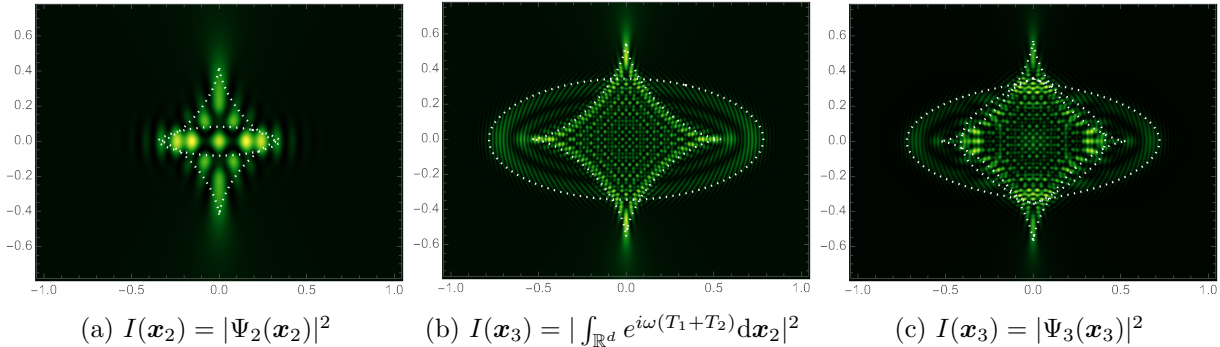
Figure 2: Example of a plasma lens with the frequency $\omega = 50$. The white dotted line is the caustic curve. *Left:* intensity pattern on the first lens-plane L_1. *Center:* single-plane approximation on the second lens-plane L_2. *Right:* double lens system.

$$= e^{i\omega(1+z_1)\frac{d_{0\,1}d_{0\,2}}{d_{1\,2}}\beta_{1\,2}\varphi_1(\boldsymbol{x}_2)} \ . \qquad (17)$$

This is a good approximation for the single image regions. Expressing the amplitude as the sum of this leading term and a term containing the details of the caustics and the interference in the multi-image regions, we write

$$\Psi_2(\boldsymbol{x}_2) = e^{i\omega T_1(\boldsymbol{x}_2,\boldsymbol{x}_2)} + \delta\Psi_2(\boldsymbol{x}_2), \qquad (18)$$

so that $\delta\Psi_2(\boldsymbol{x}_2)$ vanishes outside the interesting regions. We express the integral over $\boldsymbol{x}_2$ as the sum of a single-plane integral plus a correction which decays exponentially in the single-image regions. We then write

$$\Psi_3(\boldsymbol{x}_3) = \mathcal{N}_2\Bigg[\int_{\mathbb{R}^d} e^{i\omega(T_1(\boldsymbol{x}_2,\boldsymbol{x}_2)+T_2(\boldsymbol{x}_2,\boldsymbol{x}_3))}\mathrm{d}\boldsymbol{x}_2$$
$$+ \int_{\mathbb{R}^d} \delta\Psi_2(\boldsymbol{x}_2)e^{i\omega T_2(\boldsymbol{x}_2,\boldsymbol{x}_3)}\mathrm{d}\boldsymbol{x}_2\Bigg]. \quad (19)$$

We evaluate the first integral with Picard-Lefschetz theory, deforming the integration domain to the Lefschetz thimble $\mathcal{J}_2 \subset \mathbb{C}^d$. The second integral can be efficiently evaluated with conventional integration methods, because the perturbation $\delta\Psi_2$ renders it absolutely convergent. It is convenient to use Fast Fourier Transforms to evaluate the convolution with the Gaussian kernel $e^{i\boldsymbol{x}^2}$. We iterate this procedure till we reach the desired amplitude $\Psi(\boldsymbol{y}) = \Psi_{n+1}(\boldsymbol{y})$.

Note that this iterated integral exhibits two interesting limits. Firstly, for small separations between the lens planes $d_{i\,i+1}$, the geometric term dominates over the phase variation φ_i. In the limit where $d_{i\,i+1}$ approaches 0, the geometric term approaches a Dirac delta function in the integral, collapsing the lens planes L_i and L_{i+1} to a new plane with a phase variation $\varphi_i + \varphi_{i+1}$. Secondly, when the phase variations φ_i and φ_{i+1} of two lens planes L_i and L_{i+1} have disjoint support, the lens integral factorizes into the product of two Fresnel-Kirchhoff integrals.

Unlike the geometric approximation, the diffraction pattern of the multi-plane lens system in wave optics is sensitive to the redshifts of the lens planes z_i. The fringes in wave optics thus, in principle, provide yet another way to use lensing to probe our universe. I will study the effects of the redshifts on the fringes in a future paper.

Plasma lensing: For a further demonstration of this method, consider a two-dimensional double lens system ($d = n = 2$) with $d_{0\,1} = d_{1\,2} = d_{2\,3} = 1/3$, at low redshift $z_1 = z_2 = 0$ with the phase variation

$$\varphi_i(x,y) = \frac{1}{1 + 2x^2 + y^2}\,, \qquad (20)$$

for $i = 1,2$. See Fig. 2 for the corresponding interference patterns. Observe that the configuration of the lens-planes and their corresponding redshifts directly influence the nature of the interference pattern. The diffraction pattern of the single-lens approximation significantly deviates from the true diffraction pattern near the caustics. Moreover, the interference pattern is sensitive to the Doppler shift between the source, the lens planes, and the observer.
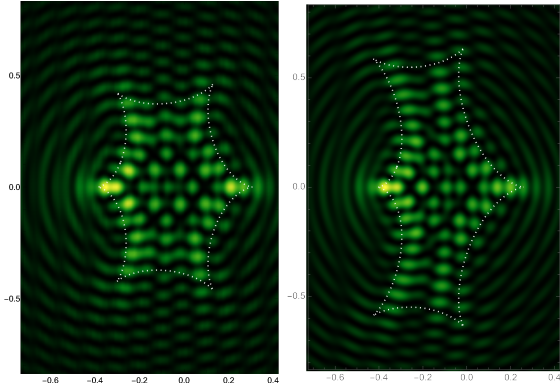
(a) Binary lens with a small radial separation.

(b) Binary lens in a single lens plane.

Figure 3: Binary system separated by an Einstein angle with the mass weightings $g_1 = \frac{1}{3}, g_2 = \frac{2}{3}$ and the frequency $\omega = 50$. The white dotted line is the caustic curve. *Left:* the masses have a small radial separation. *Right:* the masses are in a single plane (presented in [17]).

Gravitational lensing: The proposed iterative procedure works efficiently for smooth lenses. Gravitational lenses for which the phase-variation is singular are more subtle. Consider a setup with n point masses with mass M_i located at $\boldsymbol{r}_i \in L_i$ for $i = 1, \ldots, n$ with the phase variation

$$\varphi_i(\boldsymbol{x}_i - \boldsymbol{r}_i) = -g_i \log \|\boldsymbol{x}_i - \boldsymbol{r}_i\|, \qquad (21)$$

with the weighting $g_i = 4GM_i \frac{d_{0\,i} d_{i\,n+1}}{d_{0\,n+1}}$. The first integral Ψ_2 can be evaluated exactly in terms of hypergeometric functions [25]. Writing

$$\Psi_2(\boldsymbol{x}_2) = e^{-i\omega g_1 \log \|\boldsymbol{x}_2 - \boldsymbol{r}_1\|} + \delta\Psi_2(\boldsymbol{x}_2), \quad (22)$$

we express the second integral Ψ_3 as a binary single-plane lens, evaluated in elliptic coordinates [17], plus an absolutely convergent correction. See Fig. 3 for an illustration of a binary gravitational lens separated $\|\boldsymbol{r}_1 - \boldsymbol{r}_2\| = 1$, the Einstein angle, with a small radial deviation $d_{0\,1} = 0.475$, $d_{1\,2} = 0.05$, $d_{2\,3} = 0.475$. Note that both the caustic network and the diffraction pattern significantly depend on this radial displacement. (For an exploration of the caustics of gravitational binary lens systems in the geometric optics limit, see [32]).

Let's now add a third lens to the problem. If we write the amplitude

$$\Psi_3(\boldsymbol{x}_3) = e^{i\omega(T_1(\boldsymbol{x}_3,\boldsymbol{x}_3) + T_2(\boldsymbol{x}_3,\boldsymbol{x}_3))} + \delta\Psi_3(\boldsymbol{x}_3), \tag{23}$$

we cannot use Picard-Lefschetz theory for the third integral Ψ_4 due to the three singularities at $\boldsymbol{r}_1, \boldsymbol{r}_2, \boldsymbol{r}_3$ in the exponent. For the two singularities in the binary lens system, we used elliptic coordinates [17]. However, there does not exist a simple extension incorporating three foci. For this reason, we use the effective phase $-\left(\sum_{i=1}^2 g_i\right) \log \|\boldsymbol{x} - \boldsymbol{r}_m\|$ which approaches the sum $\sum_{i=1}^2 T_i$ away from the masses, with the weighted mean $\boldsymbol{r}_m = \frac{\sum_{i=1}^2 g_i \boldsymbol{r}_i}{\sum_{i=1}^2 g_i}$, to express the amplitude as

$$\Psi_3(\boldsymbol{x}_3) = e^{-i\omega \sum_{i=1}^2 g_i \log \|\boldsymbol{x}_3 - \boldsymbol{r}_m\|} + \delta\Psi_3(\boldsymbol{x}_3). \tag{24}$$

The third integral Ψ_4 is now a single-plane binary lens plus an absolutely convergent correction. This is merely a convenient representation of the calculation to add a new point mass lens. The result is still exact. We can add a fourth lens to the problem by iterating this procedure. See Fig. 4 for a demonstration of the single-plane triple gravitational lens with $d_{0\,1} = 1/2, d_{1\,2} = d_{2\,3} = 0, d_{3\,4} = 1/2$, $g_1 = g_2 = g_3 = 1/3$ forming an equilateral triangle $\boldsymbol{r}_1 = (\frac{1}{2}, -\frac{1}{2\sqrt{3}}), \boldsymbol{r}_2 = (-\frac{1}{2}, -\frac{1}{2\sqrt{3}}), \boldsymbol{r}_3 = (0, \frac{1}{\sqrt{3}})$, with sides equal to unity in terms of the Einstein angle, centered on $\frac{1}{3}(\boldsymbol{r}_1 + \boldsymbol{r}_2 + \boldsymbol{r}_3) = \boldsymbol{0}$. I used elliptic coordinates for the first two lenses and added the third lens on a separate plane in the limit $d_{2\,3} \to 0$. Note that this diffraction pattern consists of a single four-image region, six six-image regions, and a single eight-image region enclosing a ten-image region.

Conclusion: In this letter, I define and evaluate the diffraction patterns of multi-plane lensing in wave optics using a combination of Picard-Lefschetz theory and Fast Fourier Transforms. I express the integral as an iterated integral and write the intermediate integrals as the sum of a simple (unnormalized) Eikonal term and a multi-image term with compact support containing the interesting caustic and interference effects.
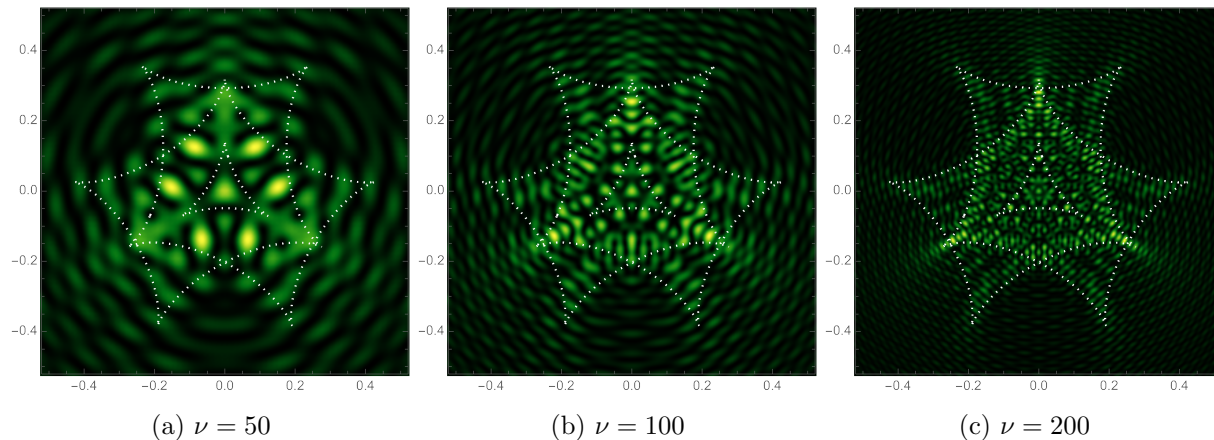
(a) $\nu = 50$ (b) $\nu = 100$ (c) $\nu = 200$

Figure 4: Triple point mass lens interference pattern for the frequencies $\omega = 50, 100$, and 200. The white dotted line is the caustic curve.

This procedure is robust and converges in polynomial time. The quantum interference is significantly richer than geometric optics near the caustics where the geometric optics approximation breaks down. The diffraction pattern contains more features and is, unlike the geometric analysis, directly sensitive to the redshifts of the lens-planes. In future work, I will perform a detailed investigation of the dependence of the fringes on the redshifts of the lens-planes. This method furthers the study on the interplay of classical catastrophe theory and interference of coherent radio sources.

[1] B. Paczynski, "Gravitational Microlensing by the Galactic Halo," *Astrophys. J.* **304** (May, 1986) 1.

[2] S. Mao and B. Paczynski, "Gravitational Microlensing by Double Stars and Planetary Systems," *Astrophysical Journal, Letters* **374** (June, 1991) L37.

[3] A. Gould and A. Loeb, "Discovering Planetary Systems through Gravitational Microlenses," *Astrophys. J.* **396** (Sept., 1992) 104.

[4] Ł. Wyrzykowski, S. Kozłowski, J. Skowron, A. Udalski, M. K. Szymański, M. Kubiak, G. Pietrzyński, I. Soszyński, O. Szewczyk, K. Ulaczyk, and R. Poleski, "The OGLE view of microlensing towards the Magellanic Clouds - III. Ruling out subsolar MACHOs with the OGLE-III LMC data," *Mon. Not. R. Astron. Soc.* **413** (May, 2011) 493–508, arXiv:1012.1154 [astro-ph.GA].

[5] S. Mao, "Astrophysical applications of gravitational microlensing," *Research in Astronomy and Astrophysics* **12** (Aug., 2012) 947–972, arXiv:1207.3720 [astro-ph.GA].

[6] B. S. Gaudi, "Microlensing Surveys for Exoplanets," *Annual Review of Astron and Astrophys* **50** (Sept., 2012) 411–453.

[7] R. Main, I. S. Yang, V. Chan, D. Li, F. X. Lin, N. Mahajan, U.-L. Pen, K. Vanderlinde, and M. H. van Kerkwijk, "Pulsar emission amplified and resolved by plasma lensing in an eclipsing binary," *Nature (London)* **557** (May, 2018) 522–525, arXiv:1805.09348 [astro-ph.HE].

[8] B. J. Rickett, "Interstellar scattering and scintillation of radio waves.," *Annual Review of Astron and Astrophys* **15** (Jan., 1977) 479–504.

[9] B. J. Rickett, "Radio propagation through the turbulent interstellar plasma.," *Annual Review of Astron and Astrophys* **28** (Jan., 1990) 561–605.

[10] R. Narayan, "The Physics of Pulsar

Scintillation," *Philosophical Transactions of the Royal Society of London Series A* **341** (Oct., 1992) 151–165.

[11] R. Blandford and R. Narayan, "Fermat's Principle, Caustics, and the Classification of Gravitational Lens Images," *Astrophys. J.* **310** (Nov., 1986) 568.

[12] A. O. Petters, H. Levine, and J. Wambsganss, *Singularity theory and gravitational lensing.* 2001.

[13] P. Schneider, J. Ehlers, and E. E. Falco, *Gravitational Lenses.* 1992.

[14] A. Gould, "Femtolensing of Gamma-Ray Bursters," *Astrophysical Journal, Letters* **386** (Feb., 1992) L5.

[15] A. Katz, J. Kopp, S. Sibiryakov, and W. Xue, "Femtolensing by dark matter revisited," *Journal of Cosmology and Astroparticle Physics* **2018** (Dec., 2018) 005, arXiv:1807.11495 [astro-ph.CO].

[16] D. L. Jow, S. Foreman, U.-L. Pen, and W. Zhu, "Wave effects in the microlensing of pulsars and FRBs by point masses," *arXiv e-prints* (Feb., 2020) arXiv:2002.01570, arXiv:2002.01570 [astro-ph.HE].

[17] J. Feldbrugge and N. Turok, "Gravitational lensing of binary systems in wave optics," *arXiv e-prints* (Aug., 2020) arXiv:2008.01154, arXiv:2008.01154 [gr-qc].

[18] A. Katz, J. Kopp, S. Sibiryakov, and W. Xue, "Looking for MACHOs in the spectra of fast radio bursts," *Mon. Not. R. Astron. Soc.* **496** (June, 2020) 564–580, arXiv:1912.07620 [astro-ph.CO].

[19] CHIME/FRB Collaboration, M. Amiri, K. Bandura, P. Berger, M. Bhardwaj, M. M. Boyce, P. J. Boyle, C. Brar, M. Burhanpurkar, P. Chawla, J. Chowdhury, J. F. Cliche, M. D. Cranmer, D. Cubranic, M. Deng, N. Denman, M. Dobbs, M. Fandino, E. Fonseca, B. M. Gaensler, U. Giri, A. J. Gilbert, D. C. Good, S. Guliani, M. Halpern, G. Hinshaw, C. Höfer, A. Josephy, V. M. Kaspi, T. L. Landecker, D. Lang, H. Liao, K. W. Masui, J. Mena-Parra, A. Naidu, L. B. Newburgh, C. Ng, C. Patel, U. L. Pen, T. Pinsonneault-Marotte, Z. Pleunis, M. Rafiei Ravandi, S. M. Ransom, A. Renard, P. Scholz, K. Sigurdson, S. R. Siegel, K. M. Smith, I. H. Stairs, S. P. Tendulkar, K. Vand erlinde, and D. V. Wiebe, "The CHIME Fast Radio Burst Project: System Overview," *Astrophys. J.* **863** (Aug., 2018) 48, arXiv:1803.11235 [astro-ph.IM].

[20] L. B. Newburgh, K. Bandura, M. A. Bucher, T. C. Chang, H. C. Chiang, J. F. Cliche,

R. Davé, M. Dobbs, C. Clarkson, K. M. Ganga, T. Gogo, A. Gumba, N. Gupta, M. Hilton, B. Johnstone, A. Karastergiou, M. Kunz, D. Lokhorst, R. Maartens, S. Macpherson, M. Mdlalose, K. Moodley, L. Ngwenya, J. M. Parra, J. Peterson, O. Recnik, B. Saliwanchik, M. G. Santos, J. L. Sievers, O. Smirnov, P. Stronkhorst, R. Taylor, K. Vanderlinde, G. Van Vuuren, A. Weltman, and A. Witzemann, "HIRAX: a probe of dark energy and radio transients," in *Ground-based and Airborne Telescopes VI*, vol. 9906 of *Society of Photo-Optical Instrumentation Engineers (SPIE) Conference Series*, p. 99065X. Aug., 2016. arXiv:1607.02059 [astro-ph.IM].

[21] J. P. Macquart, E. Keane, K. Grainge, M. McQuinn, R. Fender, J. Hessels, A. Deller, R. Bhat, R. Breton, S. Chatterjee, C. Law, D. Lorimer, E. O. Ofek, M. Pietka, L. Spitler, B. Stappers, and C. Trott, "Fast Transients at Cosmological Distances with the SKA," in *Advancing Astrophysics with the Square Kilometre Array (AASKA14)*, p. 55. Apr., 2015. arXiv:1501.07535 [astro-ph.HE].

[22] K. Vanderlinde, A. Liu, B. Gaensler, D. Bond, G. Hinshaw, C. Ng, C. Chiang, I. Stairs, J.-A. Brown, J. Sievers, J. Mena, K. Smith, K. Band ura, K. Masui, K. Spekkens, L. Belostotski, M. Dobbs, N. Turok, P. Boyle, M. Rupen, T. Landecker, U.-L. Pen, and V. Kaspi, "The Canadian Hydrogen Observatory and Radio-transient Detector (CHORD)," in *Canadian Long Range Plan for Astronony and Astrophysics White Papers*, vol. 2020, p. 28. Oct., 2019. arXiv:1911.01777 [astro-ph.IM].

[23] A. Slosar, Z. Ahmed, D. Alonso, M. A. Amin, E. J. Arena, K. Bandura, N. Battaglia, J. Blazek, P. Bull, E. Castorina, T.-C. Chang, L. Connor, R. Davé, C. Dvorkin, A. van Engelen, S. Ferraro, R. Flauger, S. Foreman, J. Frisch, D. Green, G. Holder, D. Jacobs, M. C. Johnson, J. S. Dillon, D. Karagiannis, A. A. Kaurov, L. Knox, A. Liu, M. Loverde, Y.-Z. Ma, K. W. Masui, T. McClintock, K. Moodley, M. Munchmeyer, L. B. Newburgh, C. Ng, A. Nomerotski, P. O'Connor, A. Obuljen, H. Padmanabhan, D. Parkinson, J. X. Prochaska, S. Rajendran, D. Rapetti, B. Saliwanchik, E. Schaan, N. Sehgal, J. R. Shaw, C. Sheehy, E. Sheldon, R. Shirley, E. Silverstein, T. Slatyer, A. Slosar, P. Stankus, A. Stebbins, P. T. Timbie, G. S. Tucker, W. Tyndall, F. Villaescusa Navarro,

B. Wallisch, and M. White, "Packed Ultra-wideband Mapping Array (PUMA): A Radio Telescope for Cosmology and Transients," in *Bulletin of the American Astronomical Society*, vol. 51, p. 53. Sept., 2019. `arXiv:1907.12559 [astro-ph.IM]`.

[24] E. Petroff, J. W. T. Hessels, and D. R. Lorimer, "Fast radio bursts," *Astronomy and Astrophysics Reviews* **27** (May, 2019) 4, `arXiv:1904.07947 [astro-ph.HE]`.

[25] T. T. Nakamura and S. Deguchi, "Wave Optics in Gravitational Lensing," *Progress of Theoretical Physics Supplement* **133** (Jan., 1999) 137–153.

[26] J. Feldbrugge, J.-L. Lehners, and N. Turok, "Lorentzian quantum cosmology," *Phys. Rev. D* **95** (May, 2017) 103508, `arXiv:1703.02076 [hep-th]`.

[27] J. Feldbrugge, U.-L. Pen, and N. Turok, "Oscillatory path integrals for radio astronomy," *arXiv e-prints* (Sept., 2019) arXiv:1909.04632, `arXiv:1909.04632 [astro-ph.HE]`.

[28] `https://p-lpi.github.io`.

[29] V. I. Arnol'd, "Normal forms for functions near degenerate critical points, the Weyl groups of A_k, D_k, E_k and lagrangian singularities.," *Funct. Anal. Appl.* **6** (1973) 254–272.

[30] M. V. Berry and C. Upstill, "IV Catastrophe Optics: Morphologies of Caustics and Their Diffraction Patterns," *Progess in Optics* **18** (Jan., 1980) 257–346.

[31] J. Feldbrugge, R. van de Weygaert, J. Hidding, and J. Feldbrugge, "Caustic Skeleton & Cosmic Web," *Journal of Cosmology and Astroparticle Physics* **2018** (May, 2018) 027, `arXiv:1703.09598 [astro-ph.CO]`.

[32] H. Erdl and P. Schneider, "Classification of the multiple deflection two point-mass gravitational lens models and application of catastrophe theory in lensing," *Astron. Astrophys.* **268** (Feb., 1993) 453–471.